

Launch Risk Analysis

James B. Baeker,* Jon D. Collins,† and Jerold M. Haber‡
J.H. Wiggins Company, Redondo Beach, Calif.

An analysis procedure is developed for assessing the risk associated with the launch of a missile or space booster. The method considers the various hazardous vehicle failure modes and employs a statistical characterization of the vehicle state vector following a failure; the flight termination process and the effects of the atmosphere on the fragments resulting from vehicle breakup. Based on these statistics, the impact distributions for all impacting vehicle debris are computed and used to define the impact probability and casualty expectation for locations hazarded by the launch. An incremental technique is used in these risk computations whereby fragment impact distributions are computed for discrete vehicle flight times. This allows for a considerably more accurate handling of the various sources of impact uncertainty.

Introduction

PRIOR to the launching of a missile or space booster, an assessment of the in-flight hazards posed to life and property is normally required. The resulting risk estimates indicate the location of high-risk areas and the overall level of the hazard. As a result, a launch may be postponed, a revised trajectory and/or launch vehicle configuration may be required, or high-risk locations may be partially or wholly evacuated. The hazards for an in-flight vehicle are due to impacting hardware normally jettisoned during flight or impacting vehicle fragments resulting from a malfunctioning vehicle.

Generally, the analysis of launch risk can be divided into two segments: 1) the risk for the uprange (launch area) and midrange segments of flight, and 2) the risk for the downrange (target area or re-entry) segment of flight. This paper is directed toward the analysis of risk for the uprange and mid-range flight segments.

The basic requirements of a launch risk analysis are to define the impact probability distributions for impacting vehicle debris, which account for all significant sources of impact uncertainty, and to compute the corresponding probabilities of one-or-more fragments impacting specified critical centers (land areas, generally populated) and the expectation of casualties for each center.

Analyses of the risk associated with launches have been performed prior to rocket, missile, and space booster launches for approximately 30 years. During this time, a wide variety of methods have been used by the various responsible agencies for assessing these risks. Montgomery¹ presents a discussion of the range safety function with emphasis on its application at the Eastern Test Range. The approaches applied to the range safety problem have evolved from ultra-conservative models to complex computer models which attempt to accurately account for the physics of the problem.

Hammond and Geisinger² described a comprehensive method which was the first to model the effect of a range safety destruct system on the dispersion of debris from a failed vehicle. While this method was one of the most accurate developed, it contained some limitations which would lead to significant errors in risk assessment. The launch risk methodology presented in this paper was developed to replace this method.

Collins et al.³ and Baker et al.⁴ discuss methods for predicting, in real time, the pattern of impacting debris which

would result in the event of vehicle failure and destruct. While this is a different problem from that discussed in this paper, similar types of models are required for characterizing impact uncertainties for impacting vehicle fragments.

Elements of the Problem

Before proceeding to the description of the problem solution, it is necessary to define the basic factors which must be considered. These are presented in the following paragraphs.

All significant events which can result in the impact of launch vehicle debris must be considered. This includes the normal jettisoning of hardware, such as depleted motor cases, and all modes of vehicle failure which will result in the abnormal impact of vehicle debris. The basic vehicle failure modes which are considered are malfunction turns and premature thrust termination. Malfunction turns cover all abnormal vehicle turns from a gradual turn off course to a tumble turn.

The vehicle dynamic behavior following a malfunction turn failure must be assessed to statistically define the resulting perturbation in the vehicle state vector from the time of failure to the time when steady-state conditions are reached or the vehicle breaks apart. This analysis must include the effect of a flight termination (destruct) system, if one is employed.

All fragments resulting from the breakup of a vehicle must be defined and accounted for. Breakup may result from the activation of a destruct system or may be due to excessive airloads.

The impact distribution for each fragment must include the effects of initial state vector uncertainty and the effects of the atmosphere on the fragment during freefall. State vector uncertainty results from normal vehicle guidance and control uncertainties, malfunction turn dynamics, and destruct-induced fragment velocity perturbations.

The lethality of each impacting fragment must be defined in terms of the size of the land area endangered by the fragment (casualty area) and the ability of the fragment to penetrate different classes of structures.

All endangered critical centers must be defined in terms of their location, size, and population. The distribution of the population according to various levels of sheltering must be considered.

Basic Methodology

The launch risk analysis is accomplished by segmenting the vehicle trajectory into short time intervals. Hazards for each time interval are computed for each mode of vehicle failure by assuming the failure to occur at a single representative "failure time" within the interval. For each mode of failure,

Received Feb. 2, 1977; revision received Aug. 25, 1977.

Index categories: Safety; LV/M Testing, Flight and Ground.

*Member of the Professional Staff. Member AIAA.

†Vice President. Associate Fellow AIAA.

‡Member of the Professional Staff.

the probability density distribution of the impact point is generated for each vehicle fragment resulting from the failure. The impact uncertainties are calculated based on the effects of the normal vehicle guidance and control uncertainties, failed vehicle dynamic behavior, destruct-induced velocities, wind, drag, and aerodynamic lift. Using the impact probability density distribution, the probability of impact is calculated for each fragment on each critical center. The corresponding casualty expectation is computed based on the lethality of the fragment and the expected numbers of people (by level of protection) located at the center.

The impact probabilities and casualty expectations for a given time interval and failure mode are weighted by the probability that the particular failure mode will occur during the time interval. The total impact probability (one or more fragment impacts) and casualty expectation are computed for each critical center, and for all centers, by combining the results for all failure times, failure modes, and impacting fragments. The spacing of the successive failure times for the analysis is made sufficiently close so that the successive impact distributions for each fragment overlap sufficiently to simulate the actual continuous distribution.

Details of the launch risk analysis methodology are presented in the following sections.

Fragment Impact Data

One of the primary requirements of a launch risk analysis is the computation of fragment impact data as a function of flight time. The impact data for a fragment are the coordinates (latitude and longitude) of the nominal impact point together with data required in the analysis of fragment lethality (time of fragment freefall, impact velocity components, decrease in the size of a burning solid-propellant fragment during freefall, etc.). The nominal impact point for a fragment is defined to be the impact point corresponding to an initial state vector equal to the state vector of the vehicle at the time of a failure. The mean impact point for a fragment is computed from the nominal point by applying the mean perturbations resulting from the various sources of impact uncertainty.

Since data are required for a very large number of impacting fragments (each fragment, failure mode, and failure time combination) it is necessary to employ a rapid and accurate technique for computing these data. If the impact data were computed for each impact by numerically integrating the impact trajectory, the computation time would become excessive. To overcome this problem an interpolation technique was developed which greatly reduces the required number of integrated impact computations. Integrated impact data are computed for a set of appropriately spaced vehicle flight times and fragment ballistic coefficients β . The impact data for any particular failure time and fragment (defined by its β value) are obtained by first interpolating vs flight time, followed by an interpolation vs β . Simple linear interpolations can be used

for the fragment lethality data items while cubic interpolations are required for the impact coordinates.

In addition to the computation of nominal impact data, a method is required to predict fragment impact points corresponding to relatively small perturbations in initial state vector or, equivalently, to perturbations in the vacuum impact point. To accomplish this, the concept of the "debris centerline" is used. The debris centerline (different versions of which are given in Refs. 3 and 4) is defined to be the locus of impact points for fragments having varying ballistic coefficients, corresponding to a specified initial state vector. What is required is a transformation from a known centerline, such as the centerline defined by the nominal impact points, to the perturbed centerline corresponding to a perturbed vacuum impact point. The required transformation is depicted in Fig. 1. The $\lambda' - \phi'$ coordinate system is an East-North system originating at the subvehicle point (ground-projected position of the vehicle at the time of failure) where

$$\lambda' = (\lambda - \lambda_{\text{sub}}) \cos \phi_{\text{sub}} \quad (1)$$

$$\phi' = \phi - \phi_{\text{sub}} \quad (2)$$

λ, ϕ are the longitude and latitude of impact and $\lambda_{\text{sub}}, \phi_{\text{sub}}$ are the longitude and latitude of the subvehicle point. The x - y coordinate system is defined by the "effective wind direction" which is defined to be the direction from the subvehicle point to the impact point for a fragment which immediately becomes embedded in the wind (i.e., a fragment having a very low ballistic coefficient). The direction is defined by its azimuth angle ψ . The y axis is defined to be oriented along the effective wind direction, and the x axis is rotated 90 deg clockwise from y . The transformation from the $\lambda' - \phi'$ system to the x - y system is

$$x = \lambda' \cos \psi - \phi' \sin \psi \quad (3)$$

$$y = \lambda' \sin \psi + \phi' \cos \psi \quad (4)$$

The empirical centerline transformation relations are

$$\lambda'_\beta = (I/x_{1V}) \{ (y_V - y_{1V}) \sin \psi + x_V \cos \psi \} x_{1\beta} + x_{1V} \sin \psi y_{1\beta} \quad (5)$$

$$\phi'_\beta = (I/x_{1V}) \{ (y_V - y_{1V}) \cos \psi - x_V \sin \psi \} x_{1\beta} + x_{1V} \cos \psi y_{1\beta} \quad (6)$$

Thus, given the vacuum and fragment impact points for a reference initial condition and the vacuum impact point for a perturbed initial condition, the perturbed impact point for any fragment can be predicted. The transformation provides sufficient accuracy whenever the nominal centerline is well defined.

Fragment Impact Distribution

Fragment impact uncertainties come from four basic sources: 1) uncertainty in the vehicle state vector at vehicle breakup or destruct, 2) uncertainty in any destruct velocity imparted to the fragment by a destruct system, 3) uncertainty in the atmospheric environment during freefall, and 4) uncertainty in the fragment aerodynamic lift and drag. The models associated with these uncertainties are presented in the following paragraphs. Since the sources of uncertainty are independent, e.g., wind uncertainty is independent of explosion velocity uncertainty, the effects of each uncertainty source are developed separately and then combined to produce the total impact uncertainties.

Vehicle State Vector Uncertainty

The vehicle state vector uncertainty contribution to the impact distribution is developed based on the assumption that

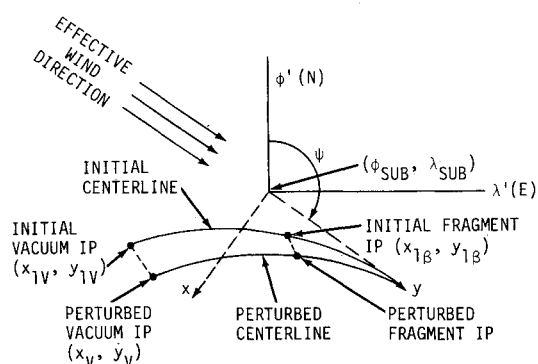


Fig. 1 Centerline transformation.

the perturbations in fragment impact points caused by variations in initial velocity (from the expected velocity) can be linearly related. Since the impacts will be assumed to be normally distributed, the probability distributions are fully characterized by the first two moments. The impact covariance matrix (defining the impact uncertainties) is calculated as shown in Eq. (7).§ The mean perturbation in the fragment impact point is obtained from the mean initial velocity perturbations $\{\Delta V\}$ as shown in Eq. (8).

$$\left[\Sigma_{DC} \right] = \left[\frac{\partial(D,C)}{\partial(V_1, V_2, V_3)} \right] \left[\Sigma_v \right] \left[\frac{\partial(D,C)}{\partial(V_1, V_2, V_3)} \right]^T \quad (7)$$

$$\left\{ \frac{\Delta D}{\Delta C} \right\} = \left[\frac{\partial(D,C)}{\partial(V_1, V_2, V_3)} \right] \left\{ \frac{\Delta V_1}{\Delta V_2}{\Delta V_3} \right\} \quad (8)$$

where

D, C = downrange and crossrange impact coordinates

V_1, V_2, V_3 = velocity components in a Cartesian coordinate system

$\left[\Sigma_{DC} \right]$ = impact covariance matrix

$\left[\Sigma_v \right]$ = initial velocity covariance matrix

The partial derivatives, referred to as miss coefficients, can be computed by perturbing the ballistic equations for a vacuum trajectory. These vacuum miss coefficients are then scaled to account for the effect of drag on an object. The scaling coefficients are determined using the centerline transformation relations, Eqs. (5) and (6).

The first source of initial velocity uncertainty to be considered is that due to guidance and performance variations of the vehicle. Frequently the effects of these variations are specified directly in terms of vacuum impact uncertainties. If these variations are defined in terms of uncertainties in the vehicle velocity vector, the uncertainties can be transformed to impact uncertainties using Eq. (7).

The most significant source of vehicle velocity uncertainty is the malfunction turn behavior of the vehicle. The turn can range from a gradual turn to a tumbling turn depending upon the effective angle of the thrust vector relative to the vehicle axis. The geometry of the turn is shown in Fig. 2. The orientation α of the tumble plane is assumed to be completely random and the angle of the thrust vector misalignment can be expressed in terms of a probability density function for the particular "gimbal" system.

To model the effect of the malfunction turn on the vehicle velocity, the effect of airloads on the vehicle during the turn were neglected. The effect of this simplification is to generate larger impact uncertainties. With this simplification, a given fixed thrust vector misalignment will result in a rotation of the vehicle velocity vector, in the tumble plane, with the angle of turn asymptotically approaching a fixed value (referred to as the steady-state velocity turn angle). The relation between the thrust vector misalignment and the steady-state turn angle is a function of the particular vehicle under consideration. It is found that the relation can be reasonably represented by the equation

$$\tan \bar{\theta} = a \delta^{-b} \quad (9)$$

§Position uncertainty can be ignored because of the relatively small influence compared to velocity uncertainty.

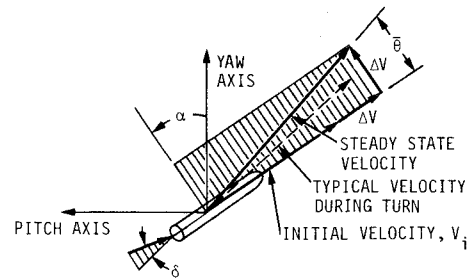


Fig. 2 Malfunction turn geometry.

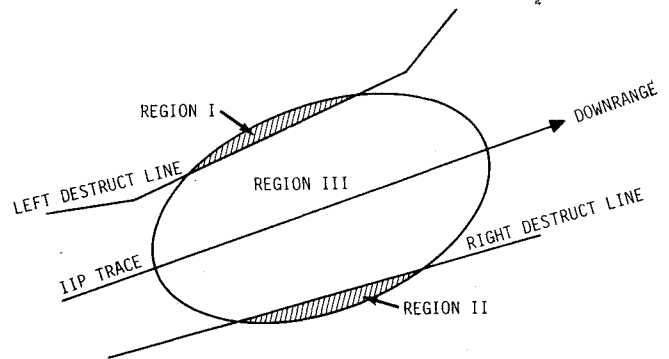


Fig. 3 Malfunction turn VIIP distribution.

where $\bar{\theta}$ is the steady-state turn angle and a and b are parameters peculiar to the vehicle. Using Eq. (9) together with the distribution on the thrust vector misalignment angle and the random orientation of the tumble plane, a joint probability density function $p(\tan \bar{\theta}, \alpha)$ is developed for the orientation of the steady-state velocity vector. The components of the incremental change in the vehicle velocity vector resulting from the malfunction turn are approximated by the relations

$$\delta V_p = \Delta V \sin \alpha \quad \delta V_y = \Delta V \cos \alpha \quad \delta V_r = \Delta V \quad (10)$$

where p, y, r refer to the pitch, yaw, and roll axes of the vehicle, respectively, and ΔV is given by

$$\Delta V = (V_i + \Delta V) \tan \bar{\theta} \approx V_i \tan \bar{\theta} \quad (11)$$

where V_i is the magnitude of the initial velocity. It has been assumed here that the velocity perturbation components along and perpendicular to the original velocity vector are equal. (In the absence of airloads these two components do, in fact, approach equality as the steady-state condition is approached.)

Using the joint probability density function $p(\tan \bar{\theta}, \alpha)$ and Eq. (10), the joint probability density function is developed for the incremental velocity components. This function is integrated to obtain the expected values and covariance matrix for these velocity components. The mean and the covariance matrix for the vacuum impact point coordinates, corresponding to the incremental velocities, are computed using vacuum miss coefficients (no drag correction) as in Eqs. (7) and (8).

The total vacuum impact uncertainties due to vehicle state vector uncertainty are now computed by adding the covariance matrices for the malfunction turn and for the guidance and performance variations. The resulting vacuum impact distribution is assumed to be bivariate normal. Fig. 3 shows an ellipse representing this distribution along with destruct lines used in making the decision to terminate vehicle flight. Normal range safety practice uses a real-time vacuum instantaneous impact point (VIIP) to determine whether a missile is malfunctioning. If this VIIP crosses a destruct

boundary, the missile is destroyed. The impact distribution as shown indicates that there is a probability that the VIIP will violate the destruct bounds. By integrating the probability density function over the regions defined by the destruct bounds (regions I, II, and III), the probability of no destruct bound violation and the probability of violation for each destruct bound are computed. Three corresponding modes of failure are defined as follows:

- left mode (region I)—vehicle VIIP violates the left destruct bound
- right mode (region II)—vehicle VIIP violates the right destruct bound
- center mode (region III)—no destruct line violations occurs

New vacuum impact means and uncertainties are computed for each of the three modes. For the center mode these are computed by integrating the original distribution over region III. The mean and uncertainties for the left and right modes are developed based on the distribution of the VIIP position as it crosses a destruct line (defined by the intersection of the destruct line with the original impact distribution), the expected velocity of the VIIP as it crosses the destruct line, and the mean and uncertainty for the time delay between destruct line violation and actual vehicle destruct.

The impact distributions for fragments, for each of the modes, are obtained from the vacuum distributions using the centerline transformation relations to relate vacuum impact perturbations to fragment impact perturbations.

Destruct-Induced Velocity

Most launch vehicles have a system which will halt powered flight upon command of a range safety controller. Typical destruct systems cut open the casing of the vehicle to relieve chamber pressure and halt thrust. This is done by explosive charges which usually produce a conflagration of flying propellant and vehicle fragments. The fragment velocities are estimated based on ground tests and flight experience and are expressed in terms of a velocity covariance matrix. The velocity covariance for each fragment is transformed to an impact covariance matrix as in Eq. (7).

Wind Uncertainty

The winds through which fragments fall can be approximated by a profile of winds, piecewise linear in altitude and direction, blowing horizontally. Statistical models of winds can be developed by selecting a set of altitudes and establishing mean values for the wind velocity components at these altitudes. Wind uncertainties can be described by a covariance matrix giving variances and covariances for the wind components for all altitudes. The wind uncertainty is derived from several sources: variability of wind, uncertainty in wind measurement, and change in the wind from the time of measurement to the time of launch.

The effect of wind uncertainty on fragment impact points can be determined by computing influence coefficients relating horizontal translation in a wind field (between two altitude levels) to wind velocity components. The influence coefficients are computed based on a fragment having a ballistic coefficient of 5 kg/m^2 ($\sim 1 \text{ psf}$) and falling embedded in the wind at terminal vertical velocity. The impact dispersions are found to vary approximately inversely with ballistic coefficient. The impact covariance for a fragment having ballistic coefficient β is thus computed as follows:

$$[\Sigma_w] = \frac{1}{\beta} [C] [\Sigma_U] [C]^T \quad (12)$$

where $[\Sigma_w]$ is the impact covariance matrix due to wind, $[C]$ is the matrix of influence coefficients, and $[\Sigma_U]$ is the wind covariance matrix.

Fragment Ballistic Coefficient Uncertainty

The ballistic coefficient ($\beta = W/C_D A$) of a particular fragment is difficult to predict because of the uncertainties in weight W , drag coefficient C_D , and cross-sectional area A . The effect of these uncertainties is to produce a curvilinear monovariate fragment impact uncertainty along the debris centerline. This dispersion may be adequately characterized by the impact points associated with the lower bound, the mean, and the upper bound estimates of the fragment β . The impact distribution is approximated by a bivariate normal distribution "fitted" to these three fragment impact points.

Fragment Lift Effects

Another source of fragment impact point uncertainty is aerodynamic lift. A spherically shaped object will fall without any lift effect, but irregularly shaped, tumbling objects will have random lift vectors. It has been established that for initial altitudes up to about 20,000 m the 1σ impact dispersion due to lift (σ_l) is approximately proportional to the initial fragment height. The proportionality constant ranges from 0.01, for blunt objects, to 0.05, for flat panel-like objects. The impact dispersion does not increase appreciably for altitudes greater than 20,000 m. Since the dispersion due to lift is random in direction, the impact covariance matrix becomes

$$[\Sigma_L] = \begin{bmatrix} \sigma_l & 0 \\ 0 & \sigma_l \end{bmatrix} \quad (13)$$

Impact Probability Computation

The total impact uncertainties for a given fragment due to a given mode of failure occurring at a particular flight time are obtained by combining the uncertainties due to the various error sources. This is done by expressing the impact covariance matrices for all error sources in a common orthogonal reference coordinate system and summing them. The resulting covariance matrix is of the form

$$[\Sigma_R] = \begin{bmatrix} \sigma_\xi^2 & \sigma_{\xi\eta} \\ \sigma_{\xi\eta} & \sigma_\eta^2 \end{bmatrix} \quad (14)$$

Based on the central limit theorem, the impact probability density function (pdf) is assumed to be approximated by a bivariate normal giving a pdf as follows:

$$p(\xi, \eta) = \frac{1}{2\pi |\Sigma_R|^{1/2}} \exp \left(-\frac{1}{2} \begin{Bmatrix} \xi \\ \eta \end{Bmatrix}^T [\Sigma_R]^{-1} \begin{Bmatrix} \xi \\ \eta \end{Bmatrix} \right) \quad (15)$$

This pdf is centered at the mean impact point for the fragment computed by shifting the nominal fragment impact point by the sum of the mean impact perturbations resulting from the impact error sources. The conditional probability of impact for the given fragment on a given critical center, given that the failure has occurred, is computed by integrating the pdf over the critical center land area.

The probability of one or more of the fragments, resulting from the given failure mode, impacting on the critical center is given by

$$P_n = 1 - \prod_{i=1}^n (1 - P_i) \quad (16)$$

where n is the number of fragments and P_i is the conditional probability of impact for the i th fragment. The probability of

one or more impacts is weighted according to the probability of occurrence of the failure mode during the time interval. The total probability of impact for a given critical center is obtained by summing the weighted probabilities of one or more impacts over all modes of failure and over all failure time intervals.

Fragment Lethality

Before proceeding to the computation of casualty expectation, it is necessary to define the various categories of impacting fragments and the lethality of these fragments to persons in various levels of sheltering.

Fragment Categories

Impacting launch vehicle fragments are divided into four categories: 1) inert pieces of vehicle structure, 2) pieces of solid propellant, 3) vehicle structures which contain propellant (solid or liquid) but are nonexplosive, and 4) fragments which contain propellant and which can explode upon impact. Definition of the fragments which will result from each type of vehicle failure are model inputs. The fragment list may vary for different segments of flight, such as for each stage of flight. For fragments which consist of or contain propellant, and which originate from a current operating booster motor, the size and weight of the fragments at vehicle breakup are adjusted according to the propellant consumed by normal operation prior to the failure. For fragments consisting of or containing burning propellant during freefall, the amount of propellant consumed prior to impact must be computed. For contained propellant, the weight of propellant consumed is computed as the product of a specified consumption rate (lb/sec) and the time of freefall. For uncontained solid-propellant fragments, the amount of propellant consumed is computed based on specified burn rate vs atmospheric pressure P relations of the form

$$\frac{dr}{dt} = AP^B \quad (\text{cm/sec}) \quad (17)$$

where dr/dt is the linear rate of burn and A and B are constants dependent on the propellant type. The propellant consumption for each propellant type is computed as part of the impact data for fragments.

Casualty Area

The casualty area of an impacting fragment is defined to be the surface area about the fragment impact point within which a person would become a casualty. The point location of both the fragment and a person are defined by their respective centroids. Casualties may result from a direct hit, from a bouncing fragment, from collapsing structure resulting from an impact on a building or other shelter, or from the overpressure pulse created by an explosive fragment.

Consider first the casualty area of a nonexplosive fragment falling vertically and impacting in the open. Let the projected area of the fragment be A_p and approximate the area occupied by a person as a circle of radius r_p . Assuming a circular fragment projected area, the fragment casualty area is given by the relation

$$A_c = \pi(\sqrt{A_p/\pi} + r_p)^2 \quad (18)$$

Since some impacting fragments would not be expected to cause significant injury due to low impact velocity and/or low fragment weight, the casualty area may be reset to zero for these fragments. The impact kinetic energy can be used as a criterion to determine whether the fragment would be expected to cause injury. Threshold kinetic energy values of from 5 to 7 kg-m have been used.

The basic casualty area expressed above should be modified to account for bouncing or scabbing upon impact and for the effect of any horizontal component of impact velocity. The

effect of a horizontal velocity component is to increase the hazarded area due to the horizontal travel of the fragment while falling from the height ($\sim 2\text{m}$) at which a person could first be struck.

The casualty area for a fragment which explodes upon impact is made up of two components as follows: 1) the overpressure zone created by the explosion; and 2) the casualty areas of propellant and hardware fragments thrown out by the explosion which impact outside of the overpressure zone. The casualty area contribution due to the fragments thrown out by the explosion is generally insignificant relative to the overpressure zone contribution and can be ignored. The casualty area due to the overpressure zone is determined by the minimum overpressure level which would be injurious to a person. The casualty area is the area of the circle whose radius is equal to the distance from the explosion at which the overpressure level has dropped to the specified level. This radius r_0 is given by the Kingery-BRL equation (Ref. 5)

$$r_0 = k_0 (fW_p)^{1/3} \quad (19)$$

where fW_p is the weight of TNT which will generate an equivalent explosion, W_p is the weight of the propellant contained in the fragment at impact, and k_0 is a factor obtained from the Kingery-BRL chart (a function of the specified overpressure level).

Adjustment for Sheltering

Thus far the casualty area computations have not accounted for the sheltering provided to persons located in structures. To do this, all sheltering is classified into predefined levels. It is assumed that that population of each critical center can be divided into the expected number of people who are unprotected and the number who are protected by each level of sheltering. People who are located in the lower floor(s) of buildings may be classified into higher levels of sheltering than those located in the upper floor(s). For nonexplosive fragments, the casualty area to sheltered persons is computed as follows:

$$A_c^* = kP_p A_c \quad (20)$$

where A_c is the casualty area of the fragment to unprotected persons (falling vertically and without bounce), k is a factor to account for the increase in the casualty area due to collapsing structure, and P_p is the probability that the fragment will penetrate the structure. P_p is based on the impact kinetic energy of the fragment and on the bounding values for the kinetic energy required to penetrate the structure.

The effect of sheltering on the casualty area for explosive fragments is accounted for by changing the minimum overpressure level upon which the overpressure zone is based. The overpressure level used is that which would be expected to severely damage or collapse the sheltering structure.

Casualty Expectation Computation

The casualty expectation for a given critical center is the number of injuries or deaths expected to result within that center from a launch.

To compute the casualty expectation for a center, due to a given failure mode and flight time interval, consider the center as being segmented into subareas A_i within which the population is afforded a constant level of sheltering. Let

P_{I_i} = probability of a given fragment impacting into subarea A_i (weighted by the probability of the failure mode occurring during the time interval)

A_{c_i} = casualty area of the fragment for the shelter level of A_i

N_i = number of people in A_i

The casualty expectation for subarea A_i is the probability of the fragment impacting in A_i times the expected number of casualties given impact. Assuming that the population in A_i is uniformly distributed, the casualty expectation is given by (Ref. 6)

$$E_{c_i} = P_{I_i} \frac{A_{c_i}}{A_i} N_i \quad (21)$$

For the critical center sufficiently small so that the fragment impact probability density over the land area A is reasonably uniform, the casualty expectation becomes

$$E_{c_i} \approx P_I \frac{A_i}{A} \frac{A_{c_i}}{A_i} N_i = P_I \frac{A_{c_i}}{A} N_i \quad (22)$$

where P_I is the probability of the fragment impacting anywhere on the center. The casualty expectation for the entire critical center is obtained by summing the E_{c_i} over all subareas. The total casualty expectation for the center is obtained by summing the individual E_c over all fragments, failure modes, and flight times.

Conclusions

Since the safety of human life and of property are of prime consideration whenever a missile or space booster is launched, it is necessary that a procedure be available for quantifying the risk. The procedure presented here provides the means for a comprehensive analysis of the risk based on normally available data. The results of this analysis can be used to establish whether the risks associated with a given operation are acceptable or to determine the range of conditions under which a given launch can occur.

This launch risk methodology has been developed into a large computer program and is currently being implemented into the range safety system at the Western Test Range (Vandenberg Air Force Base). It will be used to assess the hazards for essentially all launches from that facility. The program has been run for a variety of vehicle types including Minuteman, Scout, Atlas, Titan III and STS.

Acknowledgment

This work was developed primarily under contract to the U.S. Air Force Space and Missile Test Center (SAMTEC) and under the direction of Donald M. Benn, J.L. Jantz, and Thomas J. Froemming.

References

- ¹Montgomery, R.M., "Range Safety at the Eastern Test Range," AIAA Paper 70-246, AIAA Launch Operations Meeting, Cocoa Beach, Fla., Feb. 2-4, 1970.
- ²Hammond, W.G. and Geisinger, R.E., "Reducing Safety Constraints Through Vehicle Design," AIAA Paper 70-248, AIAA Launch Operations Meeting, Cocoa Beach, Fla., Feb. 2-4, 1970.
- ³Collins, J.D., Jameson, M., and Jantz, J.L., "Real-Time Debris Patterns for Ballistic Missile Launches," *Journal of Spacecraft and Rockets*, Vol. 13, May 1976, pp. 310-315.
- ⁴Baker, R.M.L. Jr., Mucha, T.J., Danby, D.R., Jacoby, N.H. Jr., Johnson, A.W., and Ryan, R.E., "Range Safety Debris Pattern Analysis," *The Journal of Astronautical Sciences*, Vol. XXIII, Oct.-Dec. 1975, pp. 287-323.
- ⁵Kingery, C.N. and Panhill, B.F., "Peak Overpressure vs Scaled Distance for TNT Surface Charges (Hemispherical Charge)," Ballistic Research Labs., Memo Rept. 1518, 1964.
- ⁶McMunn, J.C., Collins, J.D., and Brown, B., "A Hazards Model for Exploding Solid-Propellant Rockets," *Journal of Spacecraft and Rockets*, Vol. 6, Dec. 1969, pp. 14232-1429.

From the AIAA Progress in Astronautics and Aeronautics Series . . .

RADIATIVE TRANSFER AND THERMAL CONTROL—v. 49

Edited by Allie M. Smith, ARO, Inc., Arnold Air Force Station, Tennessee

This volume is concerned with the mechanisms of heat transfer, a subject that is regarded as classical in the field of engineering. However, as sometimes happens in science and engineering, modern technological challenges arise in the course of events that compel the expansion of even a well-established field far beyond its classical boundaries. This has been the case in the field of heat transfer as problems arose in space flight, in re-entry into Earth's atmosphere, and in entry into such extreme atmospheric environments as that of Venus. Problems of radiative transfer in empty space, conductance and contact resistances among conductors within a spacecraft, gaseous radiation in complex environments, interactions with solar radiation, the physical properties of materials under space conditions, and the novel characteristics of that rather special device, the heat pipe—all of these are the subject of this volume.

The editor has addressed this volume to the large community of heat transfer scientists and engineers who wish to keep abreast of their field as it expands into these new territories.

569 pp., 6x9, illus., \$19.00 Mem. \$40.00 List

TO ORDER WRITE: Publications Dept., AIAA, 1290 Avenue of the Americas, New York, N. Y. 10019